Bounded VNDF Sampling for Smith–GGX Reflections (Supplementary Document)

Kenta Eto
Advanced Micro Devices, Inc.
Tokyo, Japan
Kenta.Eto@amd.com

Yusuke Tokuyoshi
Advanced Micro Devices, Inc.
Tokyo, Japan
yusuke.tokuyoshi@amd.com

1 PROJECTED BOUND IN THE STRETCHED SPACE

Let an incoming direction and a microfacet normal be $\mathbf{i} = [i_x, i_y, i_z] \in \mathrm{S}^2$ and $\mathbf{m} = [m_x, m_y, m_z] \in \mathrm{S}^2$ respectively, then the reflection vector $\mathbf{o} = [o_x, o_y, o_z] \in \mathrm{S}^2$ is given by

$$\mathbf{o} = 2(\mathbf{i} \cdot \mathbf{m})\mathbf{m} - \mathbf{i}.$$

Similarly, the reflection vector in the stretched space $\acute{\mathbf{o}} = [\acute{o}_x, \acute{o}_y, \acute{o}_z] \in \mathrm{S}^2$ is

$$\acute{\mathbf{o}} = 2(\acute{\mathbf{i}} \cdot \acute{\mathbf{m}})\acute{\mathbf{m}} - \acute{\mathbf{i}},$$

where $\acute{\mathbf{i}} = [\acute{i}_x, \acute{i}_y, \acute{i}_z] \in \mathrm{S}^2$ and $\acute{\mathbf{m}} = [\acute{m}_x, \acute{m}_y, \acute{m}_z] \in \mathrm{S}^2$ are the incoming direction and the microfacet normal in the stretched space, and they are given by

$$\acute{\mathbf{i}} = \frac{[\alpha_x i_x, \alpha_y i_y, i_z]}{\left\|[\alpha_x i_x, \alpha_y i_y, i_z]\right\|}, \quad \acute{\mathbf{m}} = \frac{[m_x/\alpha_x, m_y/\alpha_y, m_z]}{\left\|[m_x/\alpha_x, m_y/\alpha_y, m_z]\right\|}.$$

In this paper, we project the tangent-space reflection vector $\mathbf{o}$ to the stretched-space reflection vector $\acute{\mathbf{o}}$. The projected $\acute{o}_z$ is obtained as follows:

$$\begin{aligned}\acute{o}_z &= 2(\acute{\mathbf{i}} \cdot \acute{\mathbf{m}})\acute{m}_z - \acute{i}_z \\ &= \frac{2m_z\left([\alpha_x i_x, \alpha_y i_y, i_z] \cdot [m_x/\alpha_x, m_y/\alpha_y, m_z]\right)}{\left\|[\alpha_x i_x, \alpha_y i_y, i_z]\right\| \left\|[m_x/\alpha_x, m_y/\alpha_y, m_z]\right\|^2} - \acute{i}_z \\ &= \frac{2m_z\,(\mathbf{i} \cdot \mathbf{m})}{\left\|[\alpha_x i_x, \alpha_y i_y, i_z]\right\| \left\|[m_x/\alpha_x, m_y/\alpha_y, m_z]\right\|^2} - \acute{i}_z.\end{aligned}$$

By substituting $\mathbf{i} \cdot \mathbf{m} = \|\mathbf{i} + \mathbf{o}\|/2$ and $[m_x, m_y, m_z] = [i_x + o_x, i_y + o_y, i_z + o_z]/\|\mathbf{i} + \mathbf{o}\|$ into the above equation, we yield

$$\acute{o}_z = \frac{(i_z + o_z)\|\mathbf{i} + \mathbf{o}\|^2}{\left\|[\alpha_x i_x, \alpha_y i_y, i_z]\right\| \left\|\left[\frac{i_x + o_x}{\alpha_x}, \frac{i_y + o_y}{\alpha_y}, i_z + o_z\right]\right\|^2} - \acute{i}_z.$$

Let $[\theta, \phi]$ be the polar coordinate of the reflection vector $\mathbf{o}$ (i.e., $o_x = \sin\theta\cos\phi$, $o_y = \sin\theta\sin\phi$, and $o_z = \cos\theta$), then we can write $\acute{o}_z$ as a function of $[\theta, \phi]$. Since $o_z = \cos\theta > 0$ for reflections, we project the lower bound of o_z (i.e., $\theta = \pi/2$) into $\acute{o}_z(\theta, \phi)$ as follows:

$$\begin{aligned}\acute{o}_z\left(\frac{2}{\pi}, \phi\right) &= \frac{i_z\|\mathbf{i} + [\cos\phi, \sin\phi, 0]\|^2}{\left\|[\alpha_x i_x, \alpha_y i_y, i_z]\right\| \left\|\left[\frac{i_x + \cos\phi}{\alpha_x}, \frac{i_y + \sin\phi}{\alpha_y}, i_z\right]\right\|^2} - \acute{i}_z \\ &= \boxed{\left(\frac{(i_x + \cos\phi)^2 + (i_y + \sin\phi)^2 + i_z^2}{\frac{(i_x + \cos\phi)^2}{\alpha_x^2} + \frac{(i_y + \sin\phi)^2}{\alpha_y^2} + i_z^2} - 1\right)\acute{i}_z}.\end{aligned} \tag{1}$$

2 DERIVATION OF OUR PDF

For the Smith–GGX mircosurface model, the previous PDF is the following visible normal distribution function (VNDF):

$$\begin{aligned}p(\mathbf{m}) &= \frac{D\,(\mathbf{m})\max\,(\mathbf{i} \cdot \mathbf{m}, 0)}{\int_{\mathrm{S}^2} D\,(\omega)\max\,(\mathbf{i} \cdot \omega, 0)\,\mathrm{d}\omega} \\ &= \frac{2D\,(\mathbf{m})\max\,(\mathbf{i} \cdot \mathbf{m}, 0)}{i_z + \sqrt{\alpha_x^2 i_x^2 + \alpha_y^2 i_y^2 + i_z^2}},\end{aligned} \tag{2}$$

where $D(\mathbf{m})$ is the GGX NDF:

$$D(\mathbf{m}) = \frac{\chi^+(m_z)}{\pi\alpha_x\alpha_y\left(\frac{m_x^2}{\alpha_x^2} + \frac{m_y^2}{\alpha_y^2} + m_z^2\right)^2}.$$

For spherical cap-based VNDF sampling [Dupuy and Benyoub 2023], the above VNDF is equivalently rewritten into the following equation:

$$p(\mathbf{m}) = q\,(\acute{\mathbf{o}})\left\|\frac{\mathrm{d}\acute{\mathbf{o}}}{\mathrm{d}\acute{\mathbf{m}}}\right\|\frac{|\det \mathbf{M}|}{\|\mathbf{M}\mathbf{m}\|^3}, \quad \text{where } \mathbf{M} = \begin{bmatrix} 1/\alpha_x & 0 & 0 \\ 0 & 1/\alpha_y & 0 \\ 0 & 0 & 1 \end{bmatrix}.$$

$q\,(\acute{\mathbf{o}})$ is the uniform distribution on the spherical cap:

$$q\,(\acute{\mathbf{o}}) = \frac{\chi^+\left(\acute{i}_z + \acute{o}_z\right)}{2\pi\left(\acute{i}_z + 1\right)}.$$

$\|\mathrm{d}\acute{\mathbf{o}}/\mathrm{d}\acute{\mathbf{m}}\| = 4|\acute{\mathbf{i}} \cdot \acute{\mathbf{m}}|$ is the Jacobian for the transformation between $\acute{\mathbf{o}}$ and $\acute{\mathbf{m}}$. $|\det \mathbf{M}|/\|\mathbf{M}\mathbf{m}\|^3$ is the Jacobian derived in Atanasov et al. [Atanasov et al. 2022]. Thus, we yield

$$\begin{aligned}\left\|\frac{\mathrm{d}\acute{\mathbf{o}}}{\mathrm{d}\acute{\mathbf{m}}}\right\|\frac{|\det \mathbf{M}|}{\|\mathbf{M}\mathbf{m}\|^3} &= \frac{4|\acute{\mathbf{i}} \cdot \acute{\mathbf{m}}|}{\alpha_x\alpha_y\left(\frac{m_x^2}{\alpha_x^2} + \frac{m_y^2}{\alpha_y^2} + m_z^2\right)^{\frac{3}{2}}} \\ &= \frac{4|\mathbf{i} \cdot \mathbf{m}|}{\alpha_x\alpha_y\left(\frac{m_x^2}{\alpha_x^2} + \frac{m_y^2}{\alpha_y^2} + m_z^2\right)^2\sqrt{\alpha_x^2 i_x^2 + \alpha_y^2 i_y^2 + i_z^2}}.\end{aligned}$$

In this paper, we replace $q\,(\acute{\mathbf{o}})$ with the uniform distribution on our spherical cap:

$$q_{\text{our}}\,(\acute{\mathbf{o}}) = \frac{\chi^+\left(k\acute{i}_z + \acute{o}_z\right)}{2\pi\left(k\acute{i}_z + 1\right)}.$$

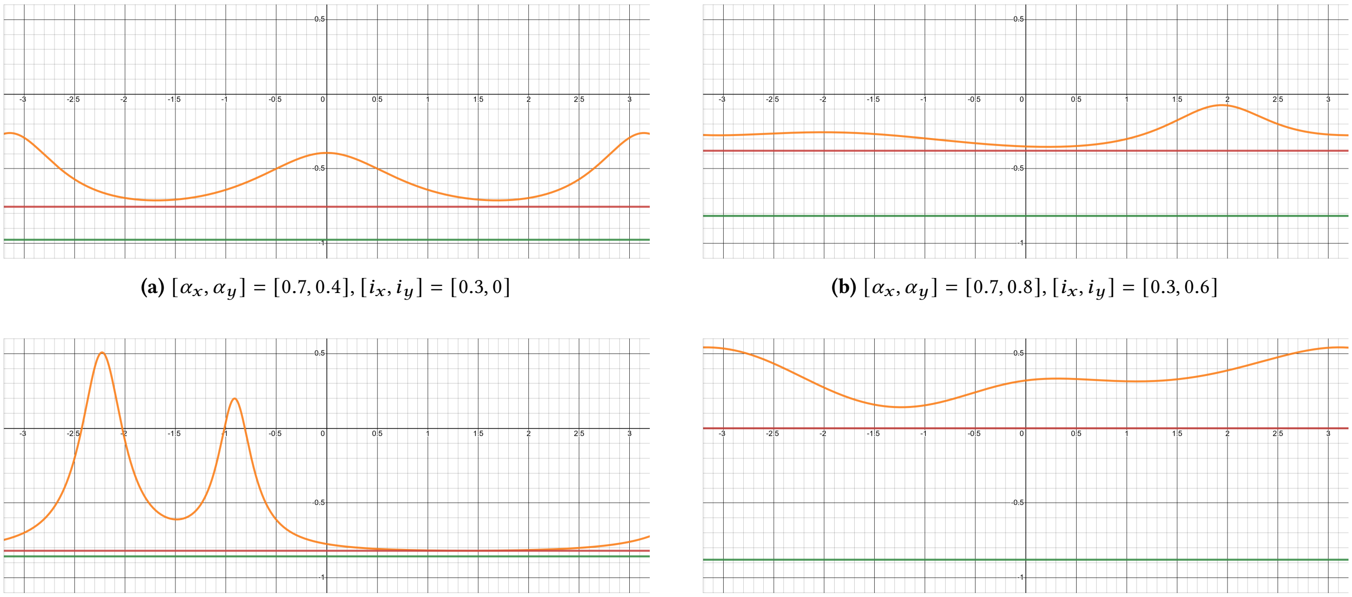

(a) $[\alpha_x, \alpha_y] = [0.7, 0.4]$, $[i_x, i_y] = [0.3, 0]$

(b) $[\alpha_x, \alpha_y] = [0.7, 0.8]$, $[i_x, i_y] = [0.3, 0.6]$

(c) $[\alpha_x, \alpha_y] = [1.5, 0.2]$, $[i_x, i_y] = [-0.2, 0.8]$

(d) $[\alpha_x, \alpha_y] = [1.6, 1.3]$, $[i_x, i_y] = [-0.2, 0.3]$

Figure 1: Plots of the previous spherical cap (green line), our spherical cap (red line), and the reflection vector bound projected into the stretched space (orange line, Eq. 1). The horizontal axis is the longitude ϕ of the tangent-space reflection vector. The vertical axis is the cosine of the spherical cap angle (i.e., $\acute{o}_z$). Our spherical cap bounds the orange line more tightly than the previous spherical cap.

Hence, the PDF for our bounded VNDF sampling is

$$p_{\text{our}}(\mathbf{m}) = q_{\text{our}}(\acute{\mathbf{o}}) \left\| \frac{\mathrm{d}\acute{\mathbf{o}}}{\mathrm{d}\acute{\mathbf{m}}} \right\| \frac{|\det \mathbf{M}|}{\|\mathbf{Mm}\|^3} = \boxed{\frac{2D(\mathbf{m}) \max(\mathbf{i} \cdot \mathbf{m}, 0)}{k i_z + \sqrt{\alpha_x^2 i_x^2 + \alpha_y^2 i_y^2 + i_z^2}} \chi^+ \left(k \acute{i}_z + \acute{o}_z\right)}.$$

3 NUMERICALLY STABLE FORM OF THE PREVIOUS PDF

When $i_z < 0$ (i.e., backfacing shading normal), our method uses the previous PDF (Eq. 2). However, if $i_z < 0$ and $\alpha_x^2 i_x^2 + \alpha_y^2 i_y^2$ is small enough compared to i_z^2, the denominator can produce catastrophic cancellation due to floating point arithmetic. This numerical error can induce zero division for the PDF. To avoid this catastrophic cancellation, we equivalently rewrite the previous PDF into the following equation:

$$\begin{aligned} p(\mathbf{m}) &= \frac{2D(\mathbf{m}) \max(\mathbf{i} \cdot \mathbf{m}, 0)}{i_z + \sqrt{\alpha_x^2 i_x^2 + \alpha_y^2 i_y^2 + i_z^2}} \\ &= \frac{2D(\mathbf{m}) \max(\mathbf{i} \cdot \mathbf{m}, 0) \left(i_z - \sqrt{\alpha_x^2 i_x^2 + \alpha_y^2 i_y^2 + i_z^2}\right)}{\left(i_z + \sqrt{\alpha_x^2 i_x^2 + \alpha_y^2 i_y^2 + i_z^2}\right)\left(i_z - \sqrt{\alpha_x^2 i_x^2 + \alpha_y^2 i_y^2 + i_z^2}\right)} \\ &= \boxed{\frac{2D(\mathbf{m}) \max(\mathbf{i} \cdot \mathbf{m}, 0) \left(\sqrt{\alpha_x^2 i_x^2 + \alpha_y^2 i_y^2 + i_z^2} - i_z\right)}{\alpha_x^2 i_x^2 + \alpha_y^2 i_y^2}}. \end{aligned}$$

Since $\sqrt{\alpha_x^2 i_x^2 + \alpha_y^2 i_y^2 + i_z^2} - i_z$ does not produce catastrophic cancellation for $i_z < 0$, we use this form in our implementation (Listing 2 in the main document).

4 INTERACTIVE VISUALIZATION OF OUR LOWER BOUND

Fig. 1 shows plots of the previous and our spherical caps using different anisotropic roughness parameters and incoming directions. Online interactive graph is available on the following URL: https://www.desmos.com/calculator/frmhvdfrno.

REFERENCES

Asen Atanasov, Vladimir Koylazov, Rossen Dimov, and Alexander Wilkie. 2022. Microsurface Transformations. *Comput. Graph. Forum* 41, 4 (2022), 105–116. https://doi.org/10.1111/cgf.14590

Jonathan Dupuy and Anis Benyoub. 2023. Sampling Visible GGX Normals with Spherical Caps. *Comput. Graph. Forum* (2023). https://doi.org/10.1111/cgf.14867